www.czasopisma.pan.pl PAN POLSKA AKADEMIA NAUK www.journals.pan.pl

Arch. Metall. Mater. **65** (2020), 1, 133-140

DOI: 10.24425/amm.2019.131106

E. SKOŁEK[1*], J. KAMIŃSKI[1], S. MARCINIAK[1], W.A. ŚWIĄTNICKI[1]

CORROSION RESISTANCE OF THE NANOSTRUCTURED X37CrMoV5-1 STEEL

The aim of this study is to compare the corrosion resistance of X37CrMoV5-l tool steel after nanostructurization and after a conventional heat treatment. The nanostructuring treatment consisted of austempering at 300°C, which produced a microstructure composed of nanometric carbide-free bainite separated by nanometric layers of retained austenite. The retained austenite occurred also in form of blocks which partially undergo martensitic transformation during final cooling. For comparison, a series of steel samples were subjected to a standard quenching and high tempering treatment, which produced a microstructure of tempered martensite. The obtained results showed that the corrosion resistance of steel after both variants of heat treatment is similar. The results indicate that the nanocrystalline structure with high density of intercrystalline boundaries do not deteriorate the corrosion resistance of steel, which depends to a greater extent on its phase composition.

Keywords: nanobainitic steel, quenched and tempered steel, TEM, EIS, polarization, corrosion

1. Introduction

The economic development requires permanent searching for new materials, technologies of their manufacturing and their treatment, allowing to decrease costs of machinery components and structures as well as increase their service life. The promising direction of steel development is producing a nanocrystalline structure in steels using phase transformations during heat treatment [1]. Properly designed heat treatment allows to produce a nanobainitic microstructure in finished components of different shapes and cross-sections [1,2]. Nanobainitic microstructure consists of nanometric bainitic ferrite laths separated by very thin layers of retained austenite. Austenite appears also in form of larger (about few micrometers) blocks. Refinement of the microstructure leads to a high strength, while the appropriate content of retained austenite in form of films guarantees good plasticity and fracture toughness. Thin films of austenite form a percolation structure and inhibit the crack propagation, while the blocks of austenite may increase the ductility and wear resistance thanks to the TRIP effect, based on the strain induced transformation of austenite into martensite [3-6].

Previous literature considerations do not give an unequivocal answer regarding the impact of a high density of intercrystalline boundaries on corrosion resistance of metallic materials. Corrosion resistance depends, to a great extent, on the kind of material, its chemical composition, corrosion environment and the type of the corrosion [3-11]. However, some trends were observed. In the case of materials with a tendency to passivate, or under conditions, in which the surface oxide layer is formed, corrosion resistance is improved with decreasing grain size, as the grain boundaries passivate faster. In the case of non-passivating materials, or conditions limiting passivation of material, with increasing the grain boundary density the reactivity of the surface increases and, consequently, the rate of corrosion increases. There are relatively few works devoted to the studies on corrosion resistance of ferrous ultrafine-grained and nanostructured steels [12,13,16-19].

The aim of the present work was to study the corrosion resistance of the X37CrMoV5-1 steel with a nanocrystalline microstructure, produced through an isothermal annealing at a temperature laying in the range of bainitic transformation. The obtained results were compared to the corrosion resistance of steel samples with the tempered martensite microstructure, produced by a conventional heat treatment consists of martensitic quenching and high tempering. The corrosion resistance has been investigated in acidic and neutral environment.

[1] WARSAW UNIVERSITY OF TECHNOLOGY, FACULTY OF MATERIALS SCIENCE AND ENGINEERING, 141 WOŁOSKA STR., 02-507 WARSZAWA, POLAND

* Corresponding author: emilia.skolek@pw.edu.pl

© 2020. The Author(s). This is an open-access article distributed under the terms of the Creative Commons Attribution-NonCommercial License (CC BY-NC 4.0, https://creativecommons.org/licenses/by-nc/4.0/deed.en which permits the use, redistribution of the material in any medium or format, transforming and building upon the material, provided that the article is properly cited, the use is noncommercial, and no modifications or adaptations are made.

2. Experimental methods

The X37CrMoV5-1 tool steel with a chemical composition presented in table 1 was austenitized at the temperature of 1030°C for 900 s, cooled down to the temperature of 300°C and annealed isothermally at this temperature in a liquid alloy of tin and silver for time needed to finish bainitic transformation. The microstructure of isothermally treated samples was investigated with the use of the transmission electron microscope TEM JEOL 1200 EX II. For microscopic observations samples were cut into thin slices, grinded to thickness of about 100μm and then electrolytic etched until their perforation. The observations were made in the bright field (BF) and dark field (DF) using reflections coming from various phases. In order to identify the phases presented in treated samples and to characterize their microstructure, the stereological analysis was performed. The width of the ferrite plates and of the austenite layers was determined according to the following stereological formula [20]:

$$d = \frac{2}{\Pi} L \tag{1}$$

where d stands for the real size of the element of the microstructure (in the analysed case the real width of a plate) and L is the size of the microstructure measured in the TEM image (in this case the width measured in the image). The plate widths (L') were measured perpendicularly to the interphase boundaries. The average width of carbide-free bainitic plates and austenite layers is defined as an arithmetic mean of 250 or more measurements of each phase. Quantitative X-ray diffraction analyses of the samples after heat treatment was conducted using CoKα radiation, within angular range of $2\theta = 140°$. The weight fractions of particular phases were determined using Rietveld refinement method exploiting Topas 4.2 software. The carbon content of retained austenite was calculated using a relationship: the lattice parameter – the carbon content in iron phases, described elsewhere [21,22].

TABLE 1

Chemical composition of X37CrMoV5-1 hot working tool steel

Element	C	Si	Mn	Cr	Mo	V	Ni	Fe
wt. %	0.37	1.01	0.38	4.91	1.2	0.34	0.19	balance

The corrosion resistance was investigated at the room temperature (22°C) by three methods: Electrochemical Impedance Spectroscopy (EIS), potentiodynamic method and gravimetric method, in the aerated solution of 0.1 M Na_2SO_4 with two levels of acidification – pH = 7 and pH = 4. Changes in pH of the solution were made with use of sulfuric acid and sodium hydroxide. The pH values were measured before the test by pH meter. Before the electrochemical measurements samples were immersed in the corrosive solutions for the time of 60 minutes. Due to the high conductivity of the electrolyte (salt solution of a strong alkali and strong acid) time of 60 minutes is enough to form and stabilize the double layer on the boundary of the metal and electrolyte and a to stabilize the corrosion potential. The EIS studies were performed in the three-electrode system with a corrosion potential within the range of frequency $10^4 \div 10^{-2}$ Hz, with a sinusoidal signal amplitude of 20 mV (in the range of –10 ÷ 10 mV). The analysis of the obtained impendence spectra was performed by means of the computer Boukamp's EQUIVCRT software. The results were presented in form of Nyquist and Bode' diagrams, showing the relationship between log $|Z|$ (where Z is a vector length on complex plane corresponding to the impedance) or an angle θ (formed by the vector "Z" of the real axis) as a function of the logarithm of frequency F. An equivalent circuits which fulfil Kramers-Kronig relationship were fitted.

The potentiodynamic studies were performed in the identical three-electrode system. Samples were polarized towards the anode from the potential 300 mV lower than the corrosion potential to the potential of 100 mV. The material was polarised with a potential change rate of 0.3 mV/s. E_{corr} and i_{corr} values were calculated from polarization curves by Tafel slopes with the use of AtlasLab software [23]. After potentiodynamic tests the surface of steel samples was observed in a Hitachi S-3500N scanning electron microscope.

The gravimetric studies were performed in compliance with the standard ASTM G31 [24]. The exposure time amounted to 12, 24 and 48 h. The obtained results were presented in the form of graphs and described, according to PH-78 / H-04608 standard [25].

3. Results and discussion

3.1. Microstructure of steel samples

The microstructure of X37CrMoV5-1 steel austempered at the temperature of 300°C, consists of carbide-free bainite with nanometric width of plates, from the range of 18 nm to 300 nm (the average width of the bainite plates is 89 nm ± 6 nm). The plates of carbide-free bainite are separated by the layers of retained austenite with a width of 4 nm to 107 nm (the average width of the austenite layers is 31 nm ± 2 nm) (Fig. 1a, 1b). In the microstructure, large blocks of retained austenite (Fig. 2a) partially transformed into martensite (Fig. 2b) are also observed. The cross-section area of austenite blocks varies from 0.13 μm^2 to 4.33 μm^2. The volume fraction of residual austenite in the sample is 19.1 ± 0.5 %. The carbon content in residual austenite is 1.168 ± 0.001 wt. %. In the microstructure a numerous of so-called midribs – a thin-plate isothermal martensite, formed in carbon rich austenite before bainitic transformation [26] and accelerating bainitic transformation [27] are observed. The hardness of the austempered steel is similar to the hardness of steel treated conventionally and amounts to 510 and 550 HV2 respectively.

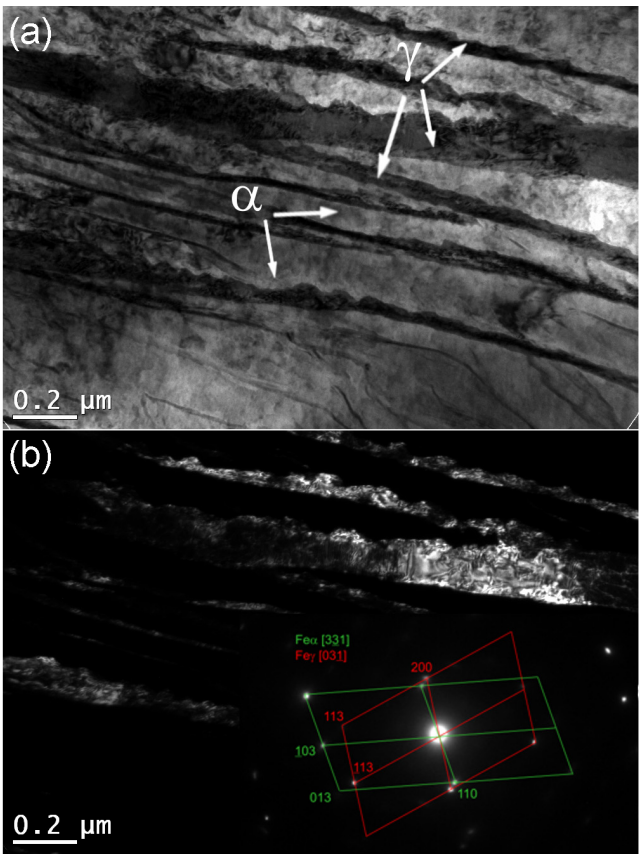

Fig. 1. Nanobainitic microstructure of X37CrMoV5-1 steel after austempering at 300°C: (a) – bright field, (b) – dark field image for (200) austenite reflection

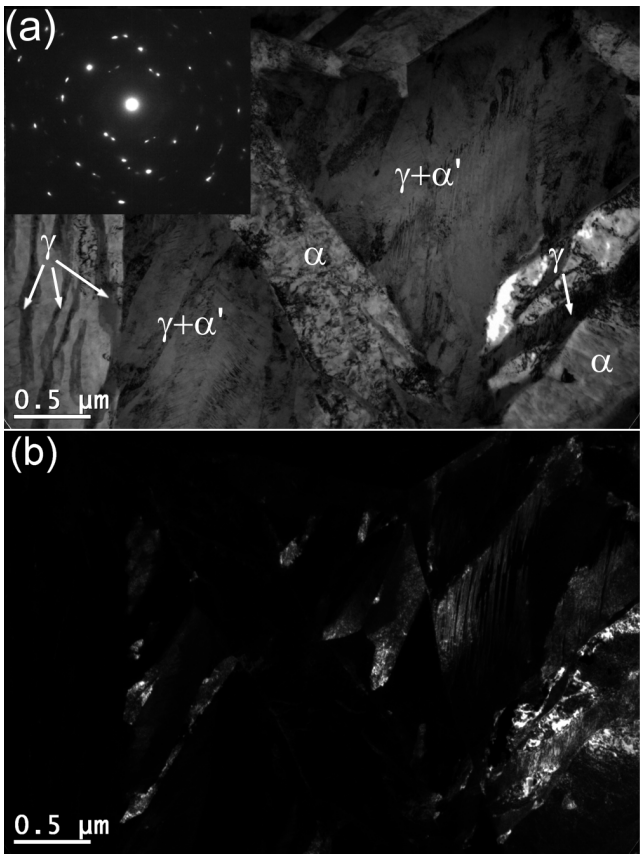

Fig. 2. The block of austenite with partial martensitic transition in X37CrMoV5-1 after austempering at 300°C: (a) – bright field, (b) – dark field image for (110) ferrite reflection

3.2. Corrosion resistance of steel

3.2.1. Results of Electrochemical Impedance Spectroscopy study

The studies on corrosion resistance by means of EIS method indicate more favourable electrochemical behaviour of the steel after nanostructurization treatment in comparison to the steel after conventional heat treatment. Regardless of the environment, for both types of treatment two capacity peaks were observed (Fig. 3a-3d), however in neutral environment these peaks overlap (Fig. 3a, 3b). The presence of two capacitive loops indicates the presence of two phases with different corrosion resistance, two different electrochemical processes or a single process that occurs with a varying intensity.

In neutral environment, irrespective of tested material, first of the processes (column 3 in table 2) is characterized by a greater resistance, an order of magnitude lower capacity and lower *n* parameter as compared to the second occurring process (column 4 in table 2. At the same time the *n* parameter of the second process (with lower resistance and higher capacity) indicates perfect resistive nature of the double layer. The estimated electrochemical

TABLE 2

Characteristic electrochemical parameters of X37CrMoV5-1 steel after various heat treatment in Na_2SO_4 neutral and acidic environment (EIS method)

Heat treatment	Parameter	pH7		pH4	
		Rp	***Rt***	***Rp***	***Rt***
	Equivalent circuit	R(RQ)(RQ)		R(RQ)(RQ)	
austempering	$R(\Omega cm^2)$	2380	1655	294	643.5
	$Y_{CPE}(F/cm^2*s^{n-1}/cm^2)$	4.20×10^{-4}	1.64×10^{-3}	4.00×10^{-4}	3.10×10^{-3}
	n	0.76	1	0.81	0.86
	Equivalent circuit	R(RQ)(RQ)		R(RQ)(RQ)	
quenching and tempering	$R(\Omega cm^2)$	1227	632	180	228
	$Y_{CPE}(F/cm^2*s^{n-1}/cm^2)$	5.78×10^{-4}	2.00×10^{-3}	5.00×10^{-4}	5.00×10^{-3}
	n	0.76	1	0.8	0.88

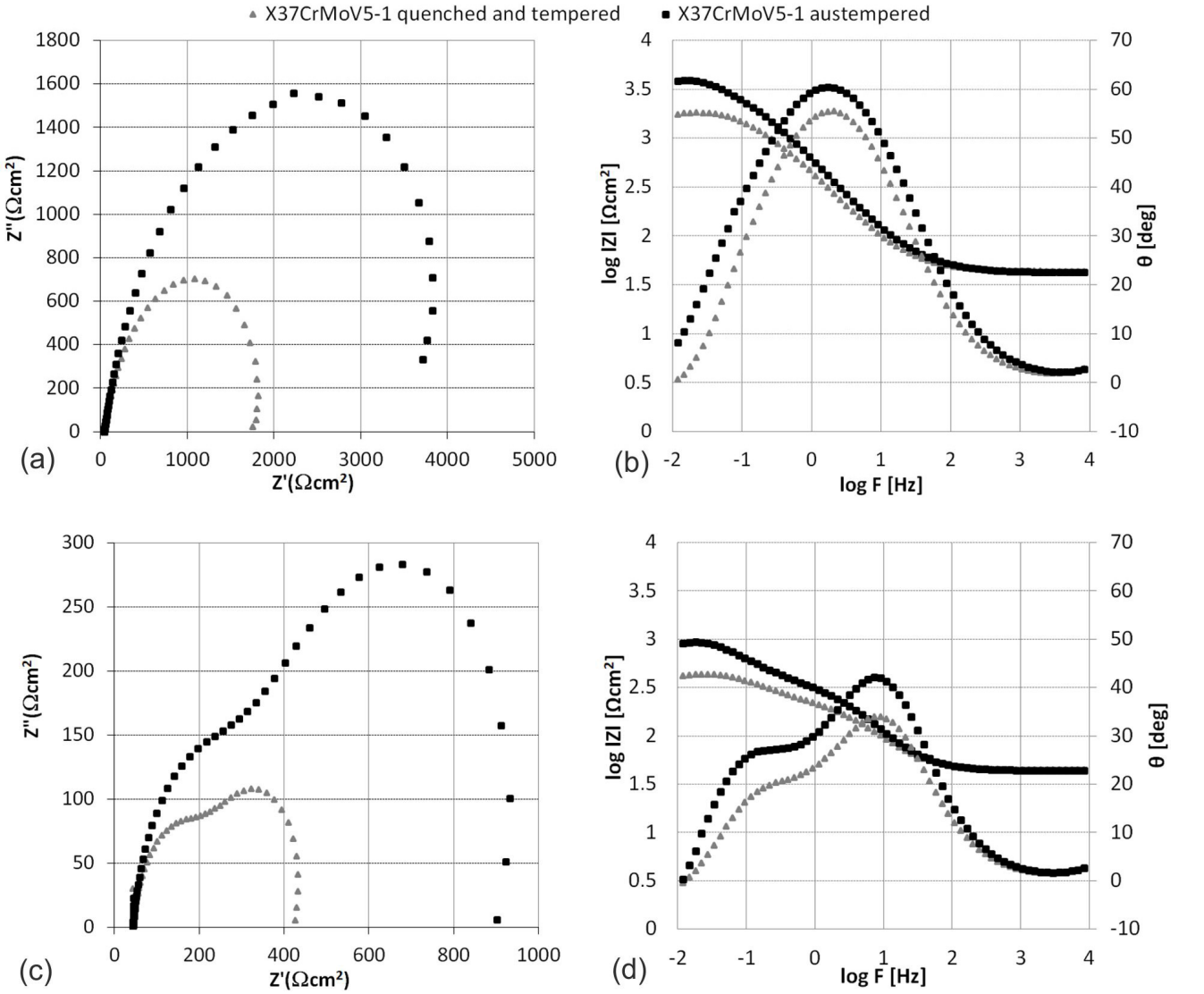

Fig. 3. Impedance spectra of X37CrMoV5-1 steel after various heat treatment: Nyquist (a) and Bode (b) diagram in neutral Na_2SO_4, Nyquist (c) and Bode (d) diagram in acidic Na_2SO_4 environment

values of both phases indicate that the phase of increased activity (n = 0.76) is characterised by an increased resistance in comparison to the less active phase (n = 1). This result may indicate an increased share of the active phase in the analysed surface, resulting the degradation of the greater part of the substrate.

In acidic environment, irrespective of tested material, the resistance value for the first process (column 5 in table 2) is slightly lower and the capacity value is an order of magnitude lower as compared to the same parameters for a second process (column 6 in table 2). Both observed phases show similar character of the double layer (n = 0.8 and n = 0.86). Low resistance values of both phases indicate intensive dissolution of the whole substrate.

3.2.2. Results of potentiodynamic tests

Fig. 4 presents polarisation curves for the heat-treated steel. The microstructure of submicron carbide-free bainite, produced by austempering, slightly improved corrosion resistance of steel samples exposed in the 0.1 M Na_2SO_4 neutral solution. The corrosion potential is shifted towards higher values as compared to the corrosion potential of X37CrMoV5-1 steel after conventional quenching and tempering treatment. Corrosion current density for both tested materials has similar value. It can be assumed, that during the tests in neutral environment, a layer of hematite, loosely bounded to the substrate and with no protective properties formed on the surface. In the acidified solution of Na_2SO_4 corrosion resistance of both steels is similar – polarization curves overlap. Such an electrochemical behaviour may resulted from a high activity of the substrate in the acidic environment and formation of a tight layer of magnetite on the surface of samples, leading to decrease the intensity of corrosion processes. In all cases, the course of polarisation curves is very approximate, typical for uniform corrosion. The shape of the curves in the cathodic area indicates that the cathodic reaction is oxygen reduction ($O_2 + 4H^+ + 4e^- \rightarrow 2H_2O$), which is controlled by diffusion.

Representative images of corrosion damage on the surface of X37CrMoV5-1 steel showed in Fig. 5a, Fig. 5c, 6b, confirm

the occurrence of general corrosion. In neutral corrosion environment, regardless the heat treatment, a local intergranular corrosion at the grain boundaries of prior austenite is also observed (Fig. 5b, d). It may indicate the segregation of alloying elements on the austenite grain boundaries during heat treatment. In acidic environment the intergranular corrosion is observed only in the case of austempering heat treatment (Fig. 6a).

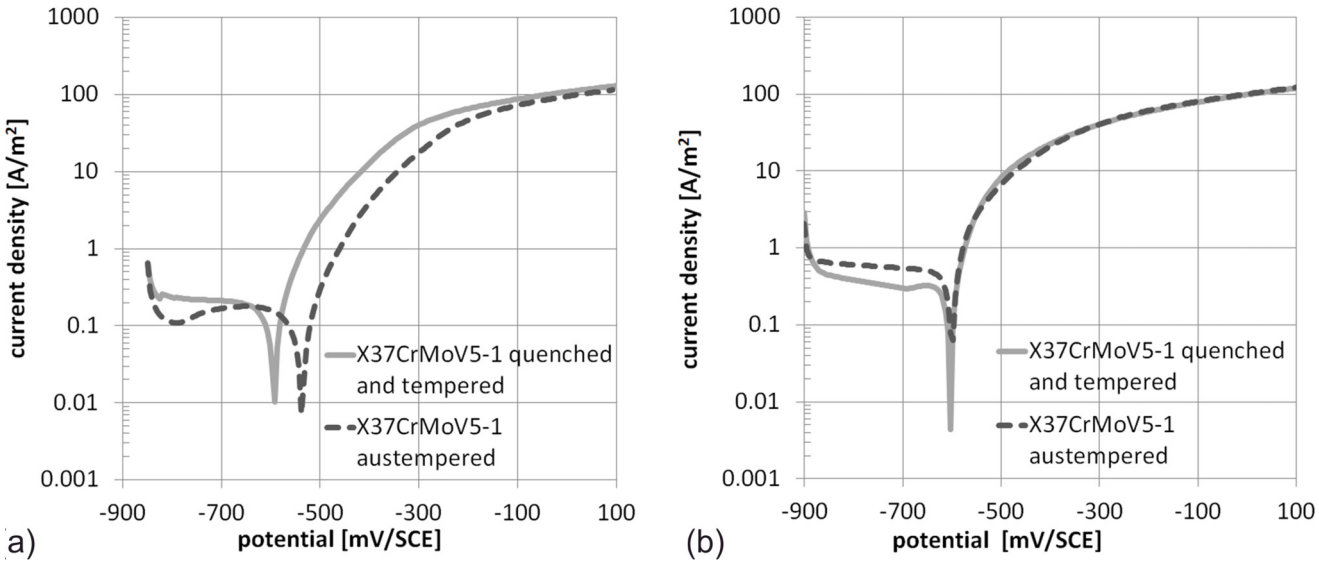

Fig. 4. Polarization curves for X37CrMoV5-1 steel after various heat treatment obtained in Na_2SO_4 neutral (a) and acidic (b) environment

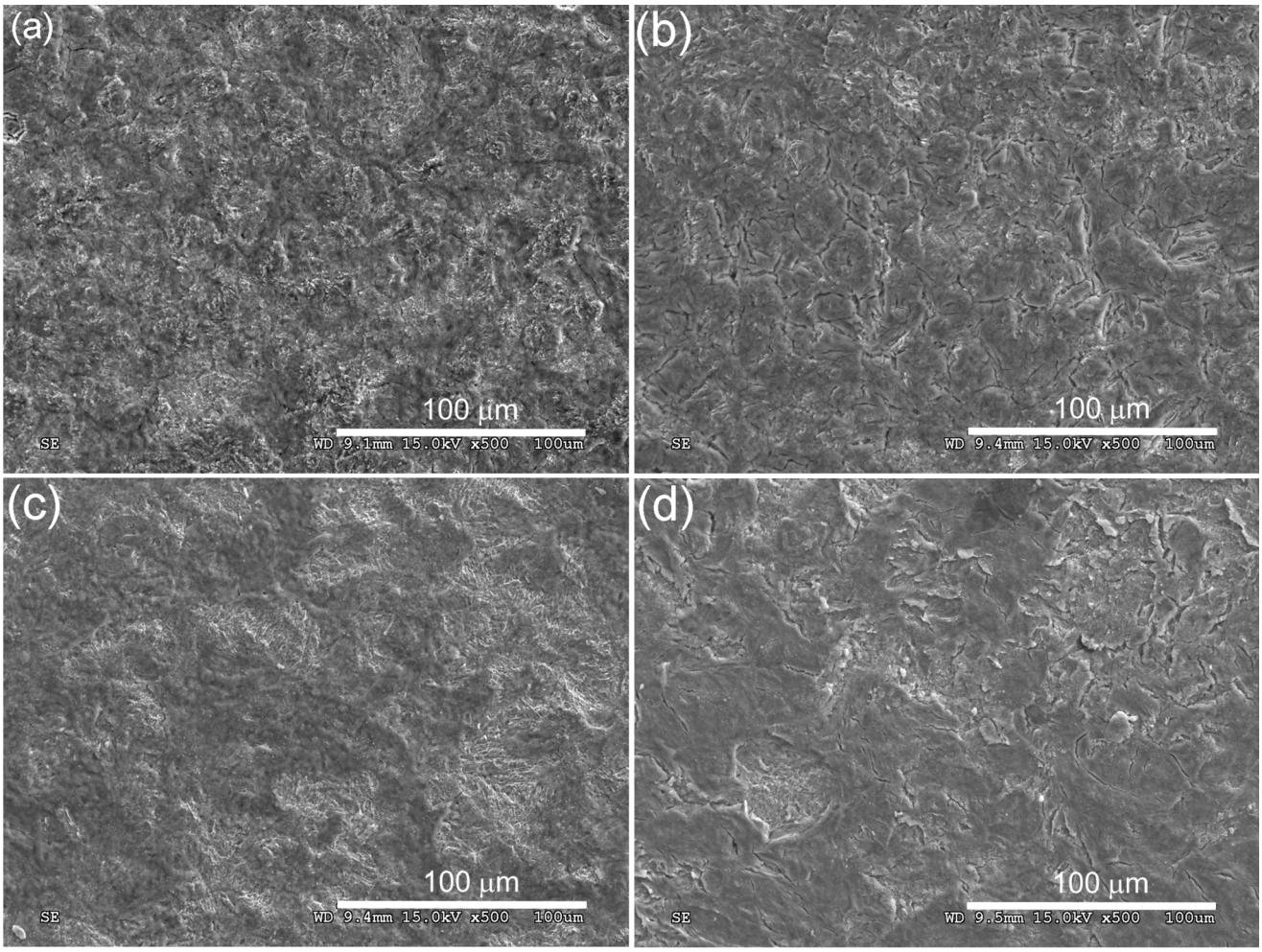

Fig. 5. Surface appearance (SEM) of X37CrMoV5-1 steel after potentiodynamic tests in Na_2SO_4 neutral environment: after austempering (a), (b), after quenching and tempering (c), (d)

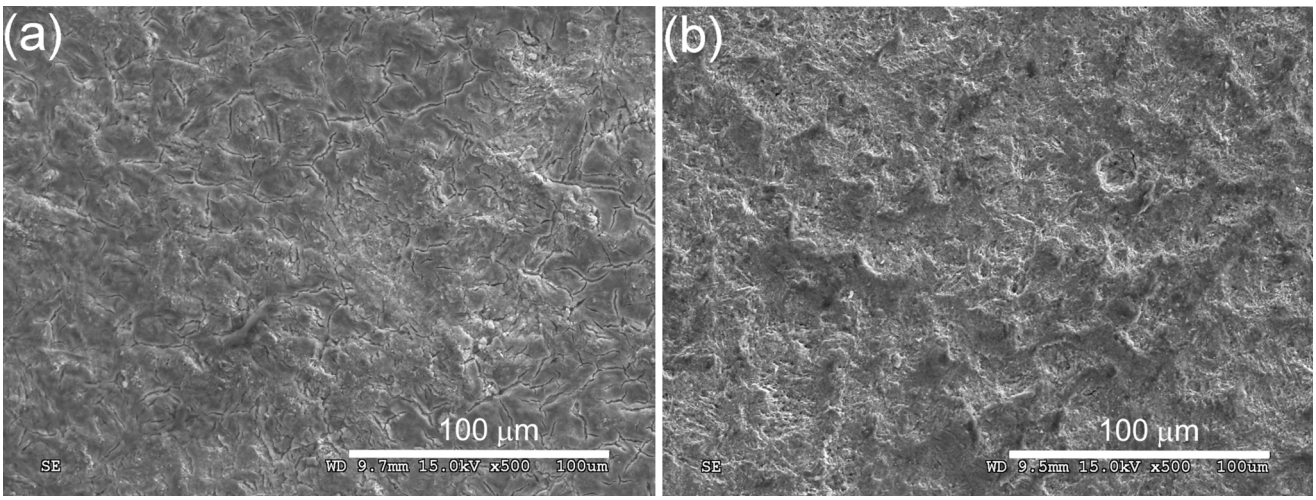

Fig. 6. Surface appearance (SEM) of X37CrMoV5-1 after potentiodynamic tests in Na_2SO_4 acidic environment: after austempering (a), after quenching and tempering (b)

TABLE 3

Characteristic electrochemical parameters of X37CrMoV5-1 steel after various heat treatment in Na_2SO_4 neutral and acidic environment (Tafel plot)

Treatment	I_{corr} [A/m^2]	E_{corr} [mV]
pH7		
austempering	0.04	–540
quenching and tempering	0.06	–590
pH4		
austempering	0.15	–600
quenching and tempering	0.11	–600

3.2.3. Results of gravimetric tests

The use of the gravimetric method does not reveal significant differences in corrosion resistance of steel samples after different variants of heat treatment in the corrosive environments (Fig. 7). The austempered steel is characterised by slightly greater corrosion resistance in comparison to the quenched and tempered steel – ca. 2% in the acidic environment (Fig. 7b) and ca. 5% in the neutral environment (Fig. 7a). The increase of the acidification of the solution causes an increase in the intensity of corrosion processes of steel, regardless of the applied treatment. Along with an increase of exposure time, the corrosion rate in the acidic environment gradually decreases This is related with a tight and well adherent layer of magnetite (Fe_3O_4), which reduces the intensity of corrosion. The increase of the thickness of the Fe_3O_4 during the test, causes the decrease of the corrosion intensity. In the neutral environment, a hematite (Fe_2O_3) layer, loosely connected with the substrate forms on the steel surface. This layer does not have barrier capabilities, as a result of which, the corrosion rate of steel samples in the neutral environment is constant in time.

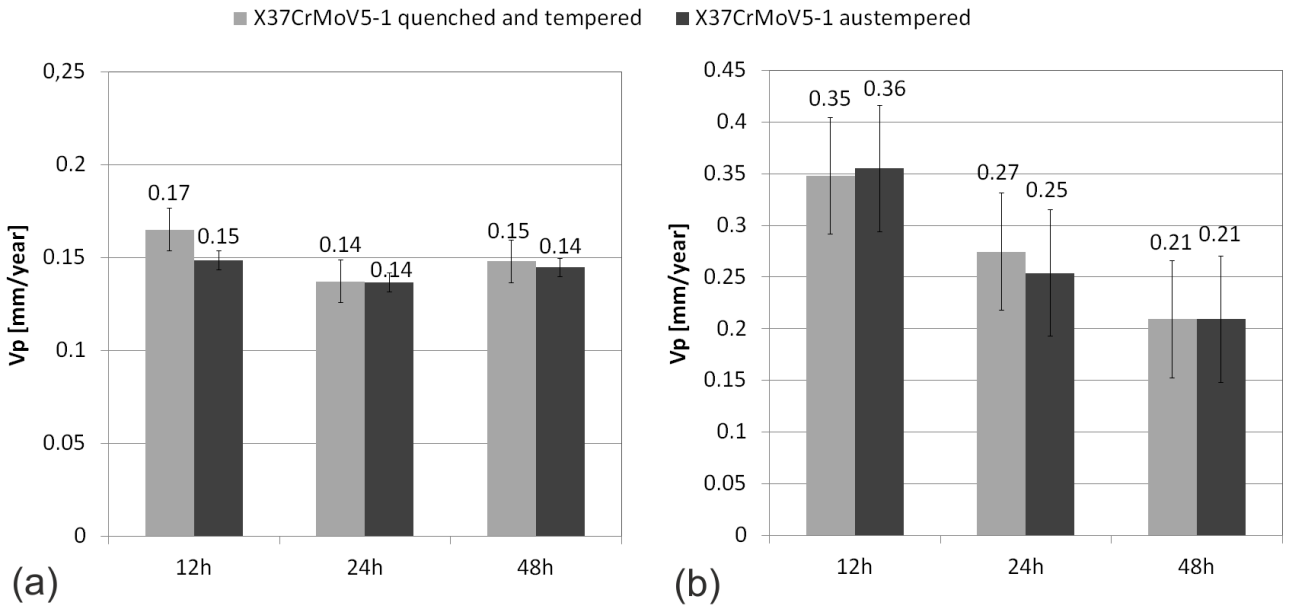

Fig. 7. Corrosion rate in Na_2SO_4 neutral (a) and acidic (b) environment of X37CrMoV5-1 steel after various heat treatment

The analysis of the scale of the corrosion resistance of tested materials, according to PH-78 / H-04608 standard shows that the investigated steel, in both types of corrosive environment, belongs to the sixth-grade of a corrosion resistance – a group of "resistant" materials. Taking into account the linear corrosion rate *Vp* (mm / year) in the neutral environment, the X37CrMoV5-1 steel after different variants of the heat treatment can be classified to a higher group of a corrosion resistance – materials "highly resistant". These are materials characterized by a linear corrosion rate in the range of *Vp* = 0.02-0.1 mm/year. In the case of the aggressive environment, especially in the case of short exposure times, the linear corrosion rate of steels classify the investigated steel to a lower group of a corrosion resistance – materials "slightly resistant", consisting of materials characterized by a linear corrosion rate in the range of *Vp* = 0.5-1 mm/year.

According to previous research carried out on the other nanocrystalline metallic materials, formation a finer microstructure leads to increase the amount of the grain boundaries, which are active areas from a point of view of corrosive attack. The activity of the grain boundaries can be considered as a positive effect – it may increase the passivation rate. On the other hand, the activity of the grain boundaries can increase the rate of unfavorable reactions of the material surface and the external environment [28].

In cast iron alloys consisting of two phases: ferrite and austenite, the influence of austenite content is also ambiguous [29,30]. On the one hand, austenite can be considered as a corrosion inhibitor [29]. On the other hand, the content of elements, such as chromium and silicon, which favor the passivation, is much smaller in austenite as compared to the ferrite [30-33]. As a result, the austenite may hardly be covered by the passive layer. Thus, an increase of the amount of austenite may have a harmful effect on corrosion resistance [30].

In dual phase steels, the corrosion resistance may also depend on the carbon content in austenite – smaller carbon saturation of austenite improves the corrosion resistance [30,31]. In our previous works [17,34] it has been shown, that the high amount of residual austenite in nanobainitic steels containing 1¸1.5% Cr and increased amount of Si or Al doesn't affect on the corrosion resistance of the samples tested in neutral and acidic Na_2SO_4 environment. Moreover, the nanostructured steel samples exhibited improved corrosion resistance in solution consisting of chloride ions [16], as compared to the conventionally heat treated samples. The investigated X37CrMoV5-1 steel contains ~1% of silicon, ~5% of chromium and approx. 19% of residual austenite in the form of layers and blocks, with high saturation of carbon. However, formation of a nanocrystalline microstructure, with a significant amount of grain boundaries, with such amount of austenite with low content of alloying elements which form a passive layer [30] and high content of carbon, does not deteriorate the corrosion resistance in aerated, aqueous acidic and neutral Na_2SO_4 solution, as compared to steel without residual austenite and lower amount of grain boundaries.

4. Summary

As result of austempering of commercial X37CrMoV5-1 steel, a nanobainitic microstructure was obtained, which consists of nanometric ferrite plates with an average grain size of 89 nm ± 6 nm separated by thin layers of retained austenite with an average grain size of 31 nm ± 2 nm.

The obtained nanocrystalline structure contains high density of intercrystalline boundaries and 19% of residual austenite.

It was revealed, that the high density of intercrystalline boundaries does not deteriorate the corrosion resistance of nanostructured steel in comparison to the steel with tempered martensite obtained by conventional heat treatment of quenching and tempering. This effect was observed for various corrosion environments. The polarization resistance measured for nanostructured steel is higher and corrosion current density, corrosion potential, corrosion rate per day and corrosion rate per year are similar as compared to the quenched and tempered steel. However, the EIS method allowed revealing the presence of two phases of different corrosion rate and various content on the tested surface.

Acknowledgments

The results presented in this paper have been obtained within the project "Production of nanocrystalline steels using phase transformations" – NANOSTAL (contract no. POIG 01.01.02-14-100/09 with the Polish Ministry of Science and Higher Education). The project is co-financed by the European Union from the European Regional Development Fund within Operational Programme Innovative Economy 2007-2013.

REFERENCES

[1] H.K.D.H. Bhadeshia, Sci. Technol. Adv. Mater. **14**, 1-7 (2013), doi:10.1088/1468-6996/14/1/014202

[2] F.G. Caballero, S. Allain, J. Cornide, J.D. Puerta Velásquez, C. Garcia-Mateo, M.K. Miller, Materials and Design **49**, 667-680 (2013), doi:10.1016/j.matdes.2013.02.046

[3] C. Garcıa-Mateo, F.G. Caballero, Materials Transactions **46**, 8, 1839-1846 (2005), https://doi.org/10.2320/matertrans.46.1839.

[4] H.K.D.H. Bhadeshia, Proc. R. Soc. A **466**, 3-18 (2010) https://doi.org/10.1098/rspa.2009.0407.

[5] H.K.D.H. Bhadeshia, Mater. Sci. Eng. A **481-482**, 36-39 (2008), doi: 10.1016/j.msea.2006.11.181.

[6] B.C. De Cooman, Current Opinion in Solid State and Materials Science **8**, 285-303 (2004), doi: 10.1016/j.cossms.2004.10.002.

[7] L.C. Chang, H.K.D.H. Bhadeshia, Materials Science and Technology **11**, 874 (1995), http://dx.doi.org/10.1179/mst.1995.11.9.874.

[8] E. Kus, Z. Lee, S. Nutt, F. Mansfeld, Corrosion **62**, 152-161 (2006), doi:10.5006/1.3278260.

[9] G.R. Argade, S.K. Panigrahi, R.S. Mishra, Corrosion Science **58**, 145-151 (2012), doi:10.1016/j.corsci.2012.01.021.

[10] A. Dischino, J.M. Kenny, Journal of Materials Science Letters **21**, 1631-1634 (2002), doi:10.1023/A:1020338103964.

[11] R. Mishra, R. Balasubramaniam, Corrosion Science **46**, 3019-3029 (2004), doi:10.1016/j.corsci.2004.04.007.

[12] H. Garbacz, M. Pisarek, K.J. Kurzydłowski, Biomolecular Engineering **24**, 559-563 (2007), doi:10.1016/j.bioeng.2007.08.007.

[13] E.S.M. Sherif, A.H. Seikh, International Journal of Electrochemical Science **7**, 7567-7578 (2012).

[14] B. Hadzimaa, M. Janeček, Y. Estrin, H.S. Kim, Materials Science and Engineering A **462**, 243-247 (2007), doi:10.1016/j.msea.2005.11.081.

[15] W. Zeiger, M. Schneider, D. Scharnweber, H. Worth, NanoStructured Materials **6**, 1013-1016 (1995).

[16] K.D. Ralston, N. Birbilis, C.H.J. Davies, Scripta Materialia **63**, 1201-1204 (2010), doi:10.1016/j.scriptamat.2010.08.035.

[17] O. Kazum, M. Bobby Kannan, H. Beladi, I.B. Timokhina, P.D. Hodgson, S. Khoddam, Materials and Design **54**, 67-71 (2014), doi:10.1016/j.matdes.2013.08.015.

[18] E. Skołek, K. Dudzińska, J. Kamiński, W. Świątnicki, Archives of Metallurgy and Materials **60**, 503-509 (2015), doi:10.1515/amm-2015-0081.

[19] E. Skołek, Sz. Marciniak, P. Skoczylas, J. Kamiński W. Świątnicki, Archives of Metallurgy and Materials **60**, 491-496 (2015), doi:10.1515/amm-2015-0079.

[20] J. Yang, Y. Lu, Z. Guo, J. Gu, C. Gu, Corrosion Science **130**, 64-75 (2018), http://dx.doi.org/10.1016/j.corsci.2017.10.027.

[21] O.D. Sherby, J. Wadsworth, D.R. Lesuer, C.K. Syn, Materials Transactions **49**, 201-2027 (2008).

[22] L. Cheng, A. Böttger, Th.H. de Keijser, E.J. Mittemeijer, Scripta Metallurgica et Materialia **24**, 509-514 (1990), https://doi.org/10.1016/0956-716X(90)90192-J.

[23] https://atlas-sollich.pl/produkt/atlaslab-software/?lang=en.

[24] ASTM G31, Standard Practice for Laboratory Immersion Corrosion Testing of Metals.

[25] PN-H-04608:1978, Korozja metali – Skala odporności metali na korozję – Polish version.

[26] M. Oka, H. Okamoto, Metallurgical and Materials Transactions A **19A**, 447-452 (1988).

[27] T.Z. Wozniak, Archives of Foundry Engineering **10**, 89-94 (2010).

[28] K.D. Ralston, N. Birbilis, Corrosion **66** (2010) 075005-075005-13, https://doi.org/10.5006/1.3462912.

[29] C.H. Hsu, M.L. Chen, Corrosion Science **52**, 2945-2949 (2010), doi:10.1016/j.corsci.2010.05.006.

[30] H. Krawiec, J. Lelito, E. Tyrała, J. Banaś, J. Solid State Electrochem. **13**, 935-942 (2009), doi:10.1007/s10008-008-0636-x.

[31] C.A. Della Rovere, F.S. Santos, R. Silva, C.A.C. Souza, S.E. Kuri, Corrosion Science **68**, 84-90 (2013), doi:10.1016/j.corsci.2012.10.038.

[32] D.Y. Kobayashi, S. Wolynec, Materials Research **2**, 239-247 (1999), http://dx.doi.org/10.1590/S1516-14391999000400002 .

[33] M. Femenia, J. Pan, C. Leygraf, Journal of The Electrochemical Society **151** (2004), B581-B585, doi: 10.1149/1.1796447.

[34] K. Wasiluk, E. Skołek, J. Kamiński, W. Świątnicki, 22nd International Conference on Materials and Technology 20-22 October 2014, Portoroz, Slovenia.